Supporting Information

Homoleptic Tris-Cyclometalated Iridium Complexes with Substituted *o*-Carboranes: Green Phosphorescent Emitters for Highly Efficient Solution-Processed Organic Light-Emitting Diodes

Yejin Kim,[†,¶] Sunghee Park,[‡,¶] Young Hoon Lee,[†] Jaehoon Jung,[†] Seunghyup Yoo,*[,‡] and Min Hyung Lee*[,†]

[†]Department of Chemistry and EHSRC, University of Ulsan, Ulsan 44610, Republic of Korea

[‡]Department of Electrical Engineering, KAIST, Daejeon 34141, Republic of Korea

Table S1. Crystallographic data and parameters for **3a** and **3c**.

	3a ·2(CH_2Cl_2)	**3c**·3($CHCl_3$)
formula	$C_{41}H_{58}B_{30}Cl_4IrN_3$	$C_{54}H_{81}B_{30}Cl_9IrN_3$
formula weight	1251.20	1607.77
crystal system	Monoclinic	Monoclinic
space group	*Cc*	*Cc*
a (Å)	13.622(3)	26.0655(5)
b (Å)	29.108(6)	23.0045(5)
c (Å)	19.170(6)	13.4263(3)
α (°)	90	90
β (°)	91.74(3)	113.347(1)
γ (°)	90	90
V (Å^3)	11561(4)	7391.5(3)
Z	8	4
ρ_{calc} (g cm^{-3})	1.438	1.445
μ (mm^{-1})	1.855	2.172
F(000)	4960	3224
T (K)	100(2)	296(2)
scan mode	ω	ϕ and ω
hkl range	–18→18, –40→40, –40→40	–32→31, –28→28, –16→16
measd reflns	59559	54444
unique reflns [R_{int}]	30976 [0.0293]	14669 [0.0648]
reflns used for refinement	30976	14669
refined parameters	1399	880
R1[a] (I > 2σ(I))	0.0303	0.0432
wR2[b] all data	0.0764	0.1020
GOF on F^2	1.024	1.068
ρ_{fin} (max/min) (e Å^{-3})	2.243/–2.799	1.162/–1.360

[a] $R1 = \sum||Fo| - |Fc||/\sum|Fo|$. [b] $wR2 = [\{\sum w(Fo^2 - Fc^2)^2\}/\{\sum w(Fo^2)^2\}]^{1/2}$.

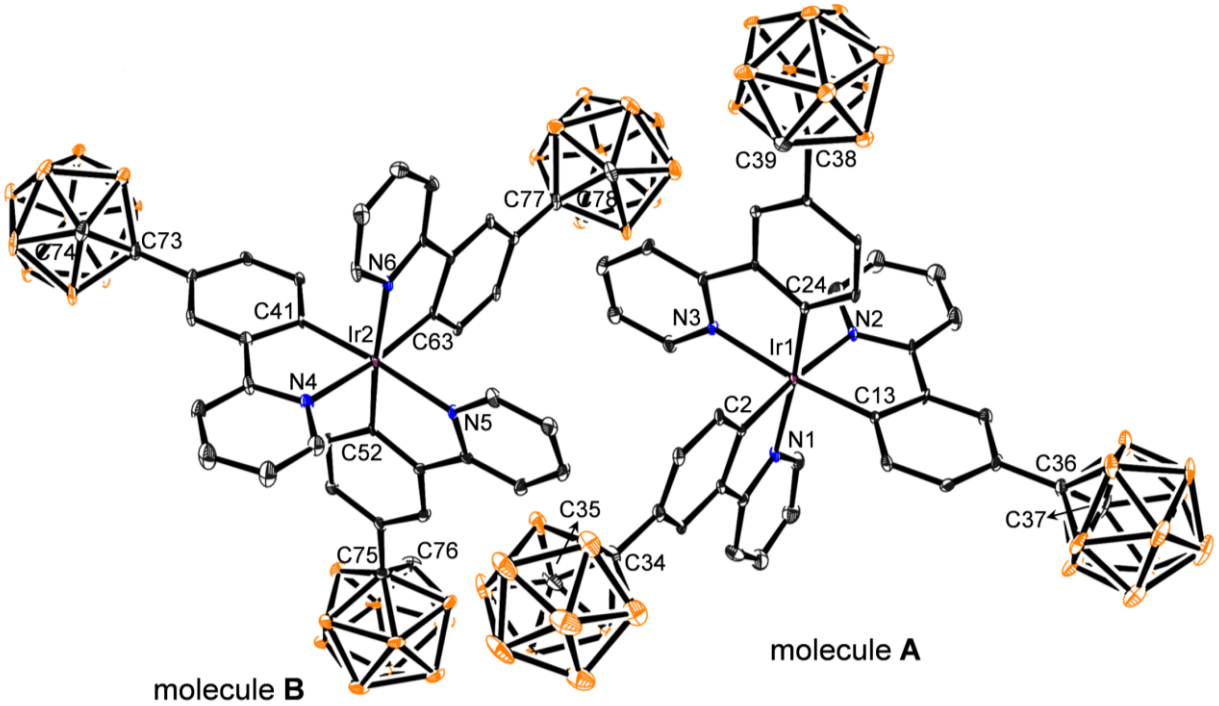

Figure S1. Crystal structures of **3a** (molecules **A** and **B**) in the asymmetric unit (40% thermal ellipsoids). The H atoms and solvent (CH_2Cl_2) molecules were omitted for clarity.

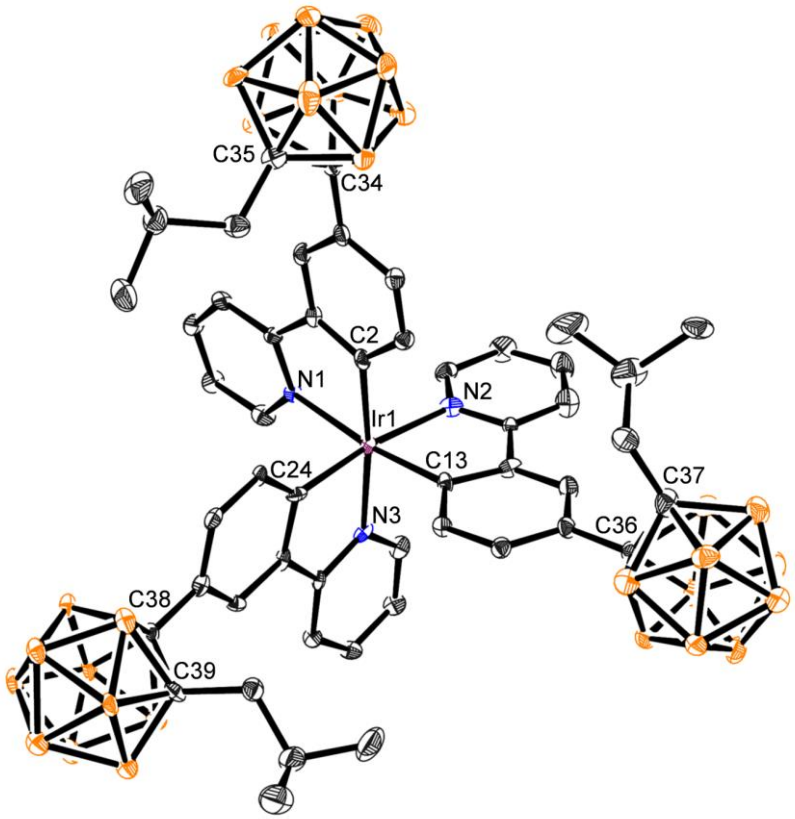

Figure S2. Crystal structure of **3c** (40% thermal ellipsoids). The H atoms and solvent ($CHCl_3$) molecules were omitted for clarity.

Table S2. Selected bond lengths (Å) and angles (deg) for **3a** and **3c**

	3a (mol **A**)		**3a** (mol **B**)		**3c**
Lengths					
Ir(1)–N(1)	2.133(4)	Ir(2)–N(4)	2.123(5)	Ir(1)–N(1)	2.140(7)
Ir(1)–N(2)	2.124(5)	Ir(2)–N(5)	2.147(4)	Ir(1)–N(2)	2.139(8)
Ir(1)–N(3)	2.138(4)	Ir(2)–N(6)	2.134(4)	Ir(1)–N(3)	2.109(8)
Ir(1)–C(2)	2.018(5)	Ir(2)–C(41)	2.009(5)	Ir(1)–C(2)	2.048(11)
Ir(1)–C(13)	2.013(5)	Ir(2)–C(52)	2.008(5)	Ir(1)–C(13)	2.015(10)
Ir(1)–C(24)	2.003(5)	Ir(2)–C(63)	2.014(5)	Ir(1)–C(24)	2.009(10)
C(34)–C(35)	1.648(9)	C(73)–C(74)	1.642(8)	C(34)–C(35)	1.729(9)
C(36)–C(37)	1.671(9)	C(75)–C(76)	1.685(9)	C(36)–C(37)	1.716(10)
C(38)–C(39)	1.689(8)	C(77)–C(78)	1.657(8)	C(38)–C(39)	1.714(9)
Angles					
C(2)–Ir(1)−N(1)	79.56(19)	C(41)–Ir(2)−N(4)	79.3(2)	C(2)–Ir(1)−N(1)	78.7(3)
C(13)–Ir(1)−N(2)	79.1(2)	C(52)–Ir(2)−N(5)	78.97(19)	C(13)–Ir(1)−N(2)	79.2(3)
C(24)–Ir(1)−N(3)	79.60(19)	C(63)–Ir(2)−N(6)	79.33(19)	C(24)–Ir(1)−N(3)	80.2(3)
C(2)–Ir(1)−N(2)	174.2(2)	C(41)–Ir(2)−N(5)	173.3(2)	C(2)–Ir(1)−N(3)	173.8(2)
C(13)–Ir(1)−N(3)	172.8(2)	C(52)–Ir(2)−N(6)	173.90(19)	C(13)–Ir(1)−N(1)	171.8(4)
C(24)–Ir(1)−N(1)	174.8(2)	C(63)–Ir(2)−N(4)	172.9(2)	C(24)–Ir(1)−N(2)	172.0(4)

Table S3. Carboranyl C–C bond distances (Å) and torsion angles (deg)

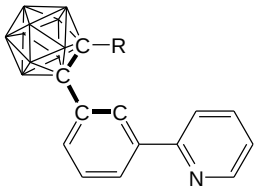

Compd (R)	C_{cage}–C_{cage} [a]	Torsion angle (ψ) [b]
3a (H)	(mol **A**) 1.648(9), 1.671(9), 1.689(8)	47.4(7), 45.5(8), 88.0(6)
	(mol **B**) 1.642(8), 1.685(9), 1.657(8)	42.1(7), 89.4(7), 44.8(7)
3c (^{i}Bu)	1.729(9), 1.716(10), 1.714(9)	91(1), 90(1), 91.1(8)

[a] C_{cage} denotes the cage carbon atoms attached to the phenyl and alkylene linker.

[b] $\psi = \angle(C_{Ph}–C_{Ph}–C_{cage}–C_{cage})$.

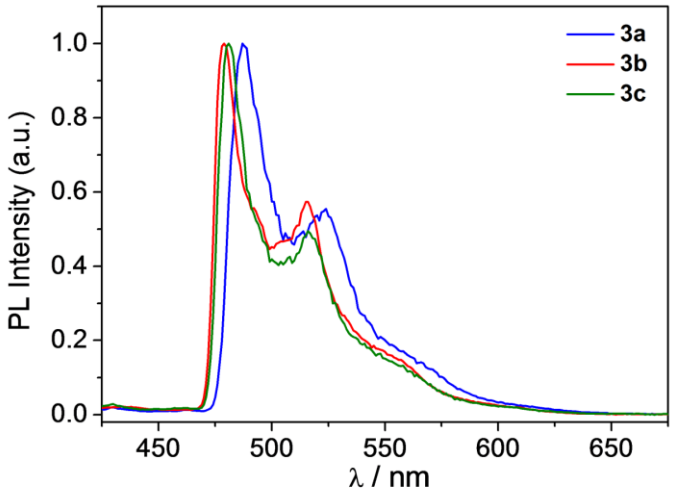

Figure S3. Normalized PL spectra of **3a**–**3c** in toluene at 77 K.

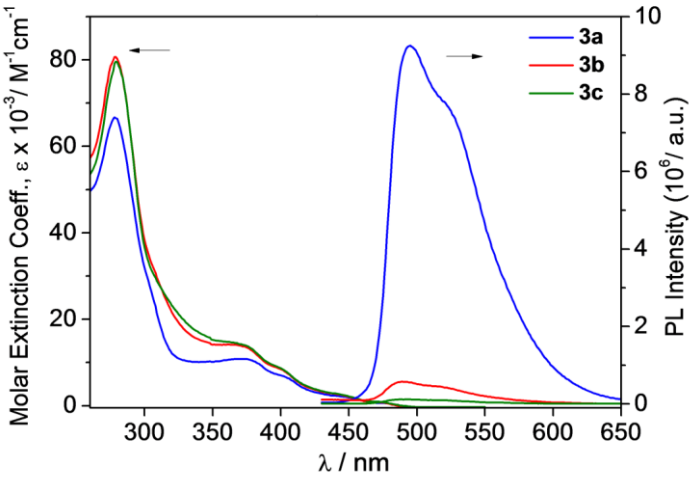

Figure S4. (Left) UV–vis absorption (5.0×10^{-5} M) and (right) PL spectra of **3a**–**3c** (1.0×10^{-5} M for **3a** and 5.0×10^{-5} M for **3b** and **3c**) in THF at 298 K.

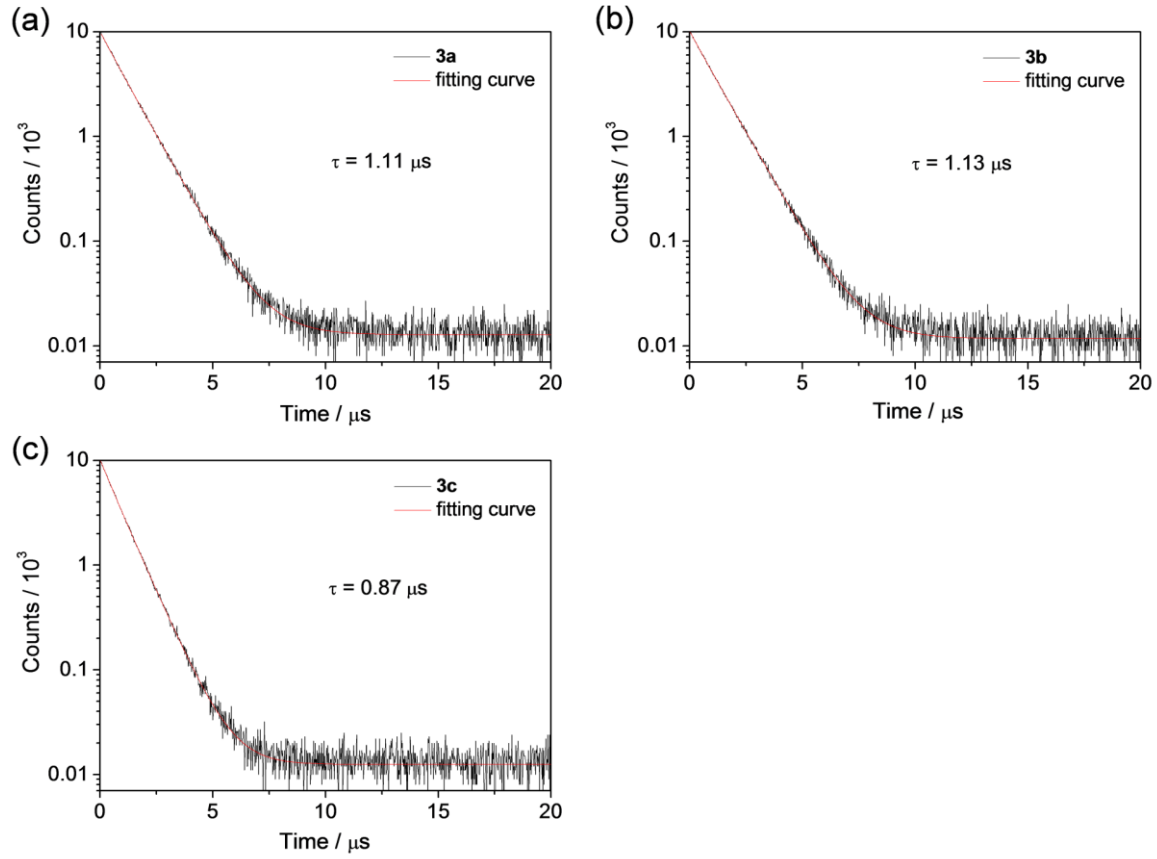

Figure S5. Emission decay curves of **3a**–**3c** in toluene at 298 K.

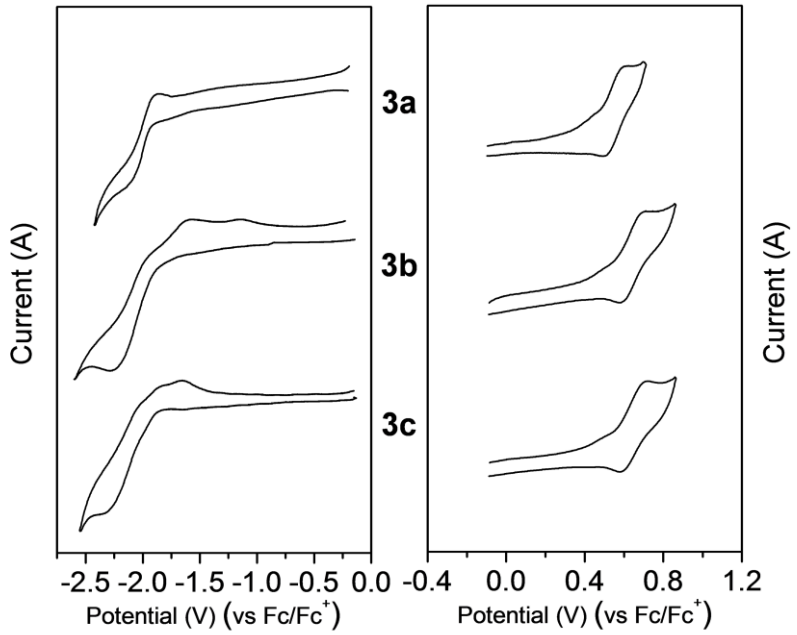

Figure S6. Cyclic voltammograms of **3a**–**3c** showing reduction (left) and oxidation (right) (5.0×10^{-4} M in DMF, scan rate = 100–200 mV/s).

DFT computational results

S_0	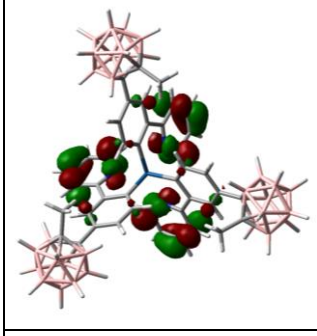	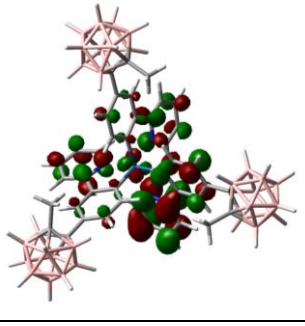	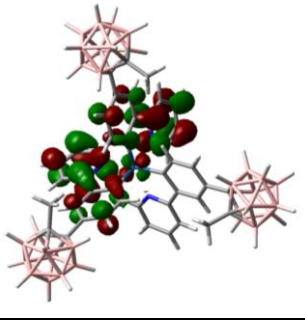	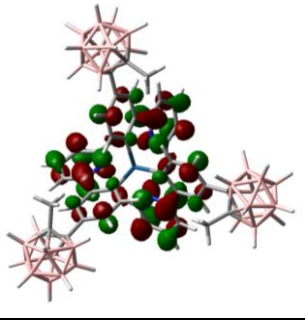
	LUMO+3	LUMO+2	LUMO+1	LUMO
	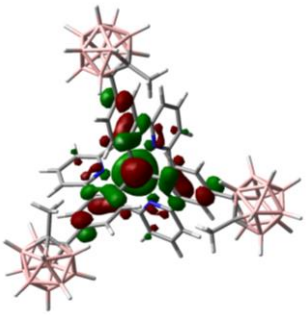	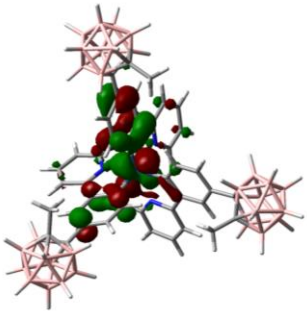	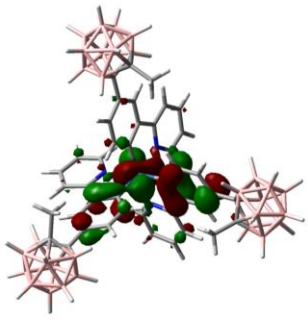	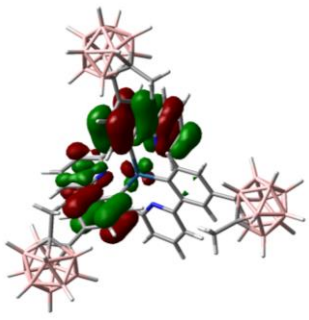
	HOMO	HOMO–1	HOMO–2	HOMO–3
T_1	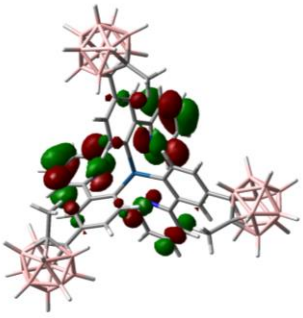	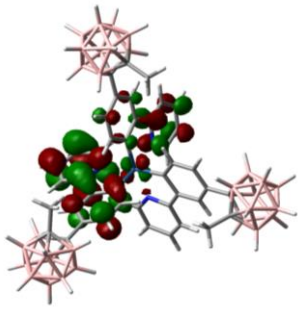	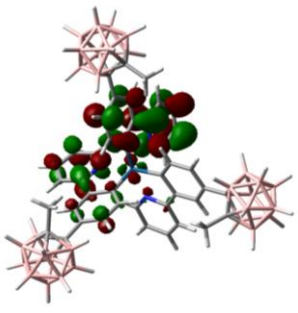	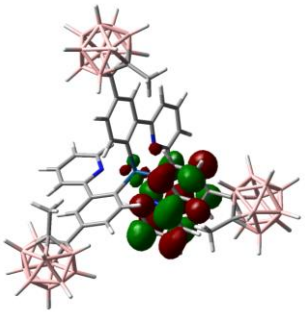
	LUMO+3	LUMO+2	LUMO+1	LUMO
	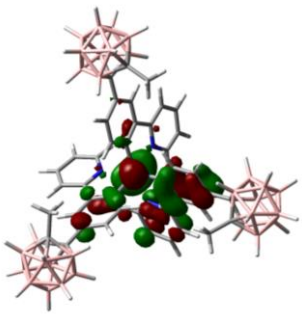	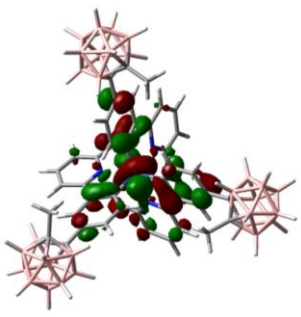	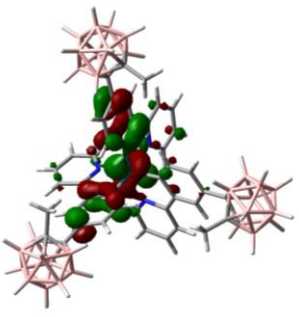	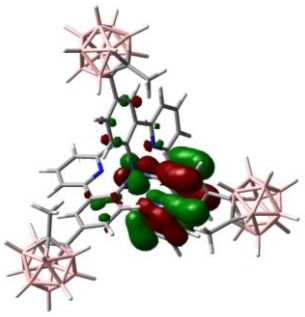
	HOMO	HOMO–1	HOMO–2	HOMO–3

Figure S7. Molecular orbitals of **3b** from B3LYP calculations with PCM in toluene at the lowest singlet ground state (S_0) and lowest triplet excited state (T_1) optimized geometries (Isovalue = 0.03).

Table S4. Molecular orbital energies (in eV) and contributions of moieties (in %) for **3b** at the ground state (S_0) optimized geometries (solvent: toluene). The contributions of MeCB moieties are presented in parentheses.

MO	Energy	Ir	Pyd1	Pyd2	Pyd3	MeCB-Ph1	MeCB-Ph2	MeCB-Ph3
LUMO+3	–1.41	1.7	26.6	28.1	26.5	5.7 (0.9)	6.1 (1.0)	5.4 (0.8)
LUMO+2	–1.74	4.2	12.2	41.0	12.6	5.9 (0.2)	18.5 (0.6)	5.7 (0.2)
LUMO+1	–1.74	4.2	33.0	0.4	32.2	15.1 (0.5)	0.2 (0.0)	15.1 (0.5)
LUMO	–1.84	1.2	19.4	23.5	19.7	11.3 (0.4)	13.5 (0.5)	11.5 (0.4)
HOMO	–5.71	51.1	3.1	3.1	3.2	13.3 (1.0)	13.0 (0.9)	13.2 (1.0)
HOMO-1	–5.84	43.3	4.3	2.2	4.3	26.9 (2.2)	3.6 (0.1)	15.4 (1.3)
HOMO-2	–5.84	43.2	3.0	5.0	2.9	3.6 (0.2)	27.1 (2.3)	15.2 (1.1)
HOMO-3	–6.66	4.4	18.7	1.9	9.8	38.3 (0.4)	2.4 (0.1)	24.6 (0.2)
HOMO-4	–6.66	4.6	1.8	17.2	11.1	6.1 (0.1)	38.9 (0.4)	20.4 (0.2)

Table S5. Molecular orbital energies (in eV) and contributions of moieties (in %) for **3b** at the lowest triplet state (T_1) optimized geometries (solvent: toluene). The contributions of MeCB moieties are presented in parentheses.

MO	Energy	Ir	Pyd1	Pyd2	Pyd3	MeCB-Ph1	MeCB-Ph2	MeCB-Ph3
LUMO+3	–1.37	1.7	35.8	12.4	32.8	8.1 (1.3)	3.0 (0.6)	6.2 (0.9)
LUMO+2	–1.74	3.8	16.9	0.6	47.8	7.4 (0.2)	0.3 (0.0)	23.2 (0.8)
LUMO+1	–1.78	2.9	45.8	2.5	15.6	23.8 (0.8)	1.2 (0.1)	8.3 (0.3)
LUMO	–2.12	2.9	1.9	53.1	1.2	1.0 (0.0)	38.7 (1.1)	1.2 (0.1)
HOMO	–5.64	44.8	2.0	10.6	2.0	4.0 (0.2)	24.1 (1.5)	12.6 (0.9)
HOMO-1	–5.84	40.3	3.5	6.7	3.4	17.4 (1.4)	17.7 (1.3)	11.1 (0.8)
HOMO-2	–5.87	43.2	4.0	2.6	4.3	23.1 (1.7)	3.8 (0.2)	19.1 (1.6)
HOMO-3	–6.53	14.0	2.8	25.5	2.3	4.5 (0.1)	46.5 (0.5)	4.5 (0.2)

Table S6. Computed absorption and phosphorescence emission wavelengths (λ_{calc} in nm) and contributions of metal-to-ligand charge transfer (MLCT, in %) to the transition for **3b** from TD-B3LYP calculations at the ground (S_0) and lowest triplet state (T_1) optimized geometries, respectively.

State	$\lambda_{calc.}$/ nm	$f_{calc.}$	Major contribution	MLCT (%)
S1	397.7	0.0084	HOMO→LUMO (97.3%)	49.9
S2	390.1	0.0053	HOMO→LUMO+1 (95.0%)	46.9
S3	389.8	0.0054	HOMO→LUMO+1 (94.8%)	46.9
S4	374.9	0.0542	HOMO-1→LUMO (90.9%)	42.1
S5	374.1	0.0615	HOMO-2→LUMO (91.0%)	42.0
T1	491.1[a]	0.0000	HOMO→LUMO (67.4%)	41.9
			HOMO-3→LUMO (14.3%)	11.1
			HOMO-1→LUMO (11.1%)	37.4

[a] For the adiabatic transition corresponding to the 0–0 phosphorescence.

S_0	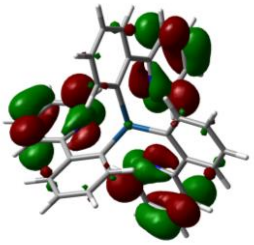	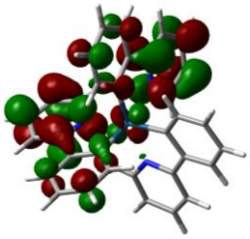	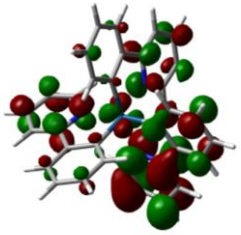	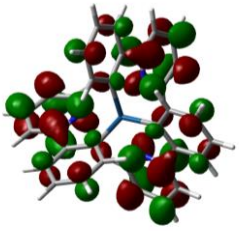
	LUMO+3	LUMO+2	LUMO+1	LUMO
	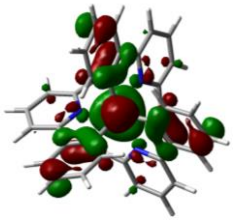	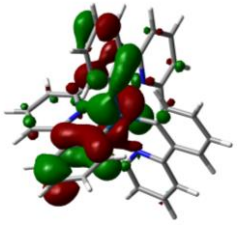	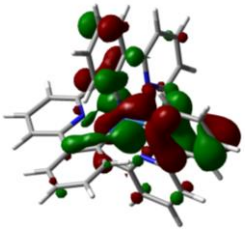	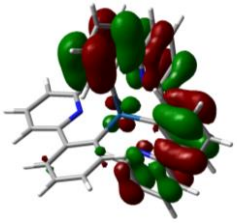
	HOMO	HOMO−1	HOMO−2	HOMO−3

T_1	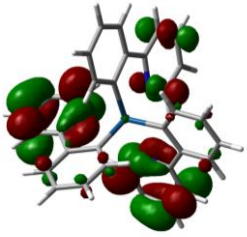	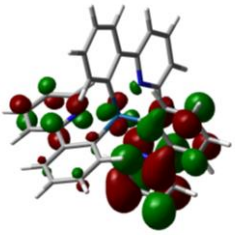	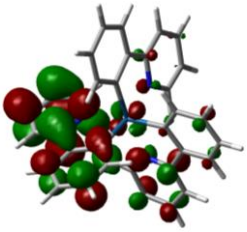	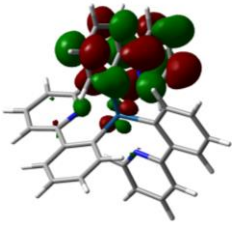
	LUMO+3	LUMO+2	LUMO+1	LUMO
	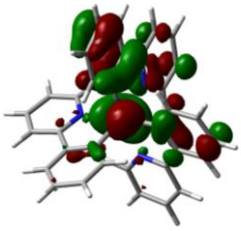	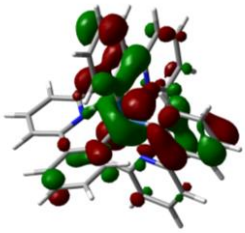	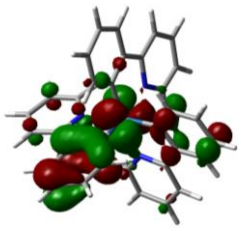	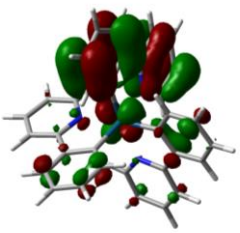
	HOMO	HOMO−1	HOMO−2	HOMO−3

Figure S8. Molecular orbitals of **4** from B3LYP calculations with PCM in toluene at the lowest singlet ground state (S_0) and lowest triplet excited state (T_1) optimized geometries (Isovalue = 0.03).

Table S7. Molecular orbital energies (in eV) and contributions of moieties (in %) for **4** at the ground state (S_0) optimized geometries (solvent: toluene).

MO	Energy	Ir	Pyd1	Pyd2	Pyd3	Ph1	Ph2	Ph3
LUMO+3	–0.89	2.1	29.1	29.4	29.2	3.4	3.5	3.3
LUMO+2	–1.16	4.5	36.5	0.4	34.2	12.6	0.2	11.7
LUMO+1	–1.16	4.6	11.5	46.5	13.1	4.0	15.8	4.5
LUMO	–1.26	1.2	22.5	23.7	23.1	9.6	10.1	9.8
HOMO	–4.97	51.1	3.0	2.9	2.9	13.8	13.5	12.8
HOMO-1	–5.10	42.9	2.8	2.6	4.9	17.8	2.4	26.7
HOMO-2	–5.10	42.9	4.0	4.2	2.0	13.1	28.6	5.2
HOMO-3	–5.96	3.3	14.3	11.0	0.5	42.0	26.4	2.5
HOMO-4	–5.96	3.3	2.9	6.1	16.8	5.3	20.5	45.1

Table S8. Molecular orbital energies (in eV) and contributions of moieties (in %) for **4** at the lowest triplet state (T_1) optimized geometries (solvent: toluene).

MO	Energy	Ir	Pyd1	Pyd2	Pyd3	Ph1	Ph2	Ph3
LUMO+3	–0.85	2.1	12.4	34.1	41.5	1.1	3.9	4.9
LUMO+2	–1.17	4.0	0.8	59.6	10.6	0.3	21.2	3.5
LUMO+1	–1.21	3.3	3.0	9.6	57.3	1.3	4.0	21.4
LUMO	–1.48	3.2	57.3	1.6	2.7	32.8	1.2	1.2
HOMO	–4.90	45.8	8.6	1.9	2.0	24.9	13.2	3.7
HOMO-1	–5.11	40.4	6.5	3.3	2.4	19.5	18.5	9.3
HOMO-2	–5.14	43.3	1.6	3.6	4.6	2.6	11.9	32.3
HOMO-3	–5.89	9.2	22.9	3.2	2.5	48.5	7.1	6.5

Table S9. Computed absorption and phosphorescence emission wavelengths (λ_{calc} in nm) and contributions of metal-to-ligand charge transfer (MLCT, in %) to the transition for **4** from TD-B3LYP calculations at the ground (S_0) and lowest triplet state (T_1) optimized geometries, respectively.

State	$\lambda_{calc.}$/ nm	$f_{calc.}$	Major contribution	MLCT (%)
S1	420.0	0.0107	HOMO→LUMO (97.0%)	50.0
S2	412.4	0.0046	HOMO→LUMO+1 (95.0%)	46.6
S3	412.4	0.0043	HOMO→LUMO+2 (94.9%)	46.6
S4	393.3	0.0454	HOMO-1→LUMO (89.1%)	41.7
S5	393.0	0.0449	HOMO-2→LUMO (88.8%)	41.7
T1	508.7[a]	0.0000	HOMO→LUMO (73.1%])	42.6

[a] For the adiabatic transition corresponding to the 0–0 phosphorescence.

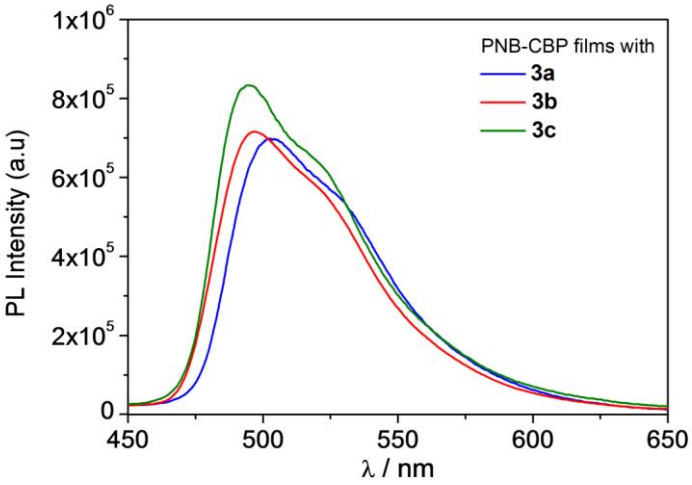

	λ_{PL} (nm)	Φ_{PL} (%)
3a	503	32 (±1.80)
3b	496	33 (±0.75)
3c	495	36 (±0.73)

Figure S9. PL spectra of PNB-CBP film doped with **3a**–**3c** (8 wt% of Ir).

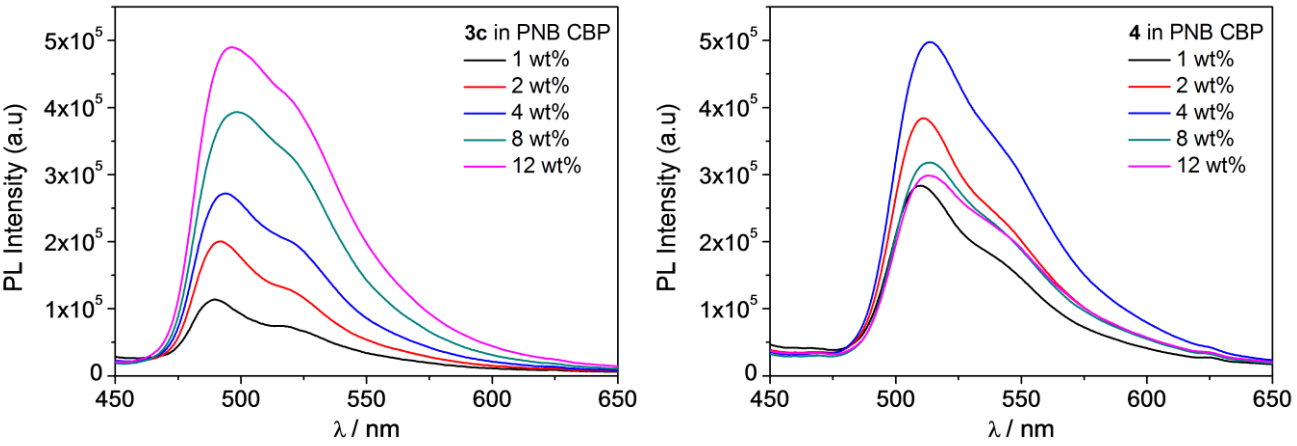

Figure S10. PL spectra of PNB-CBP film doped with **3c** (left) and **4** (right) (Table 3 in the main text).

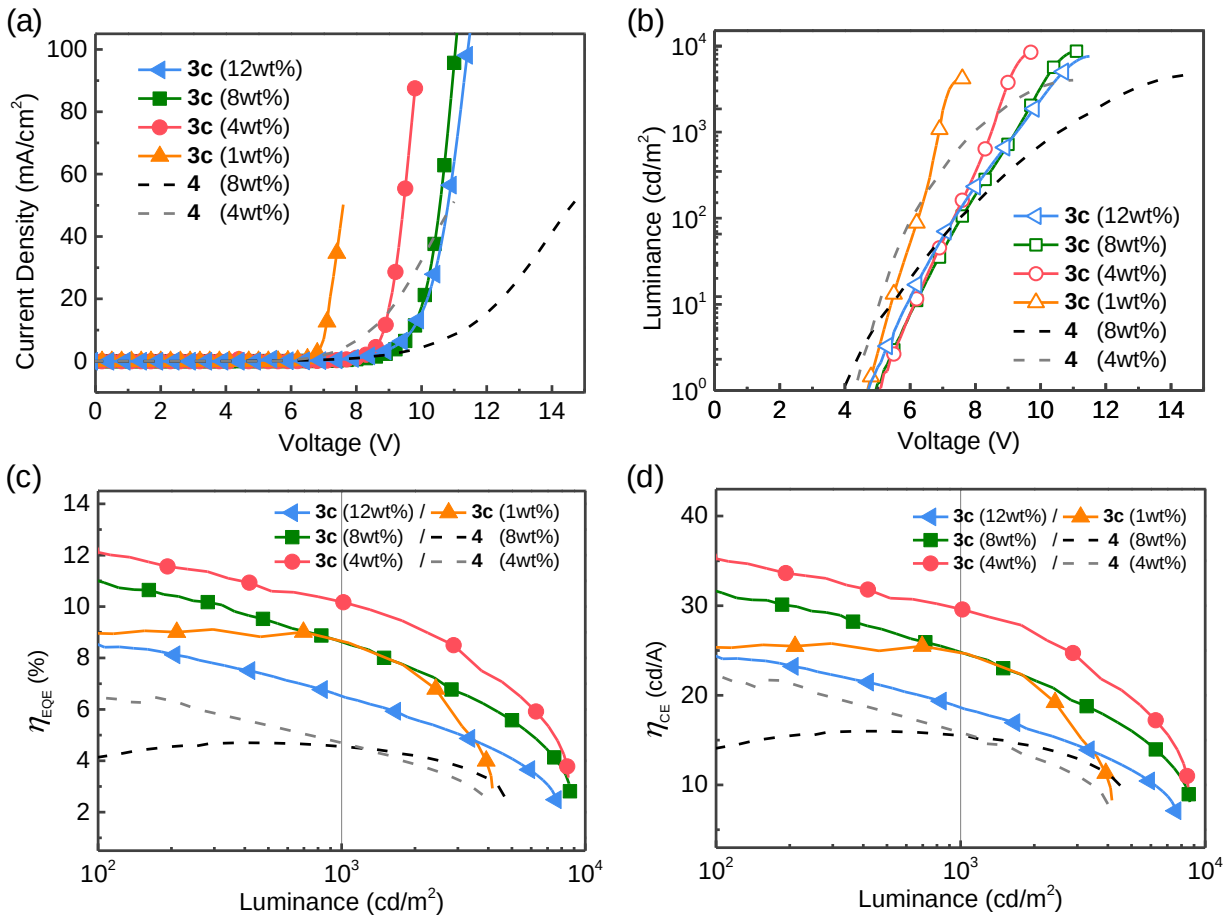

Figure S11. (a) Current density-voltage (*J*–*V*), (b) luminance-voltage (*L*–*V*), (c) external quantum efficiency-luminance (η_{EQE}–*L*), and (d) current efficiency-luminance (η_{CE}–*L*) curves of devices (**D3c-I**–**D3c-IV** and **D4-I**–**D4-II**).

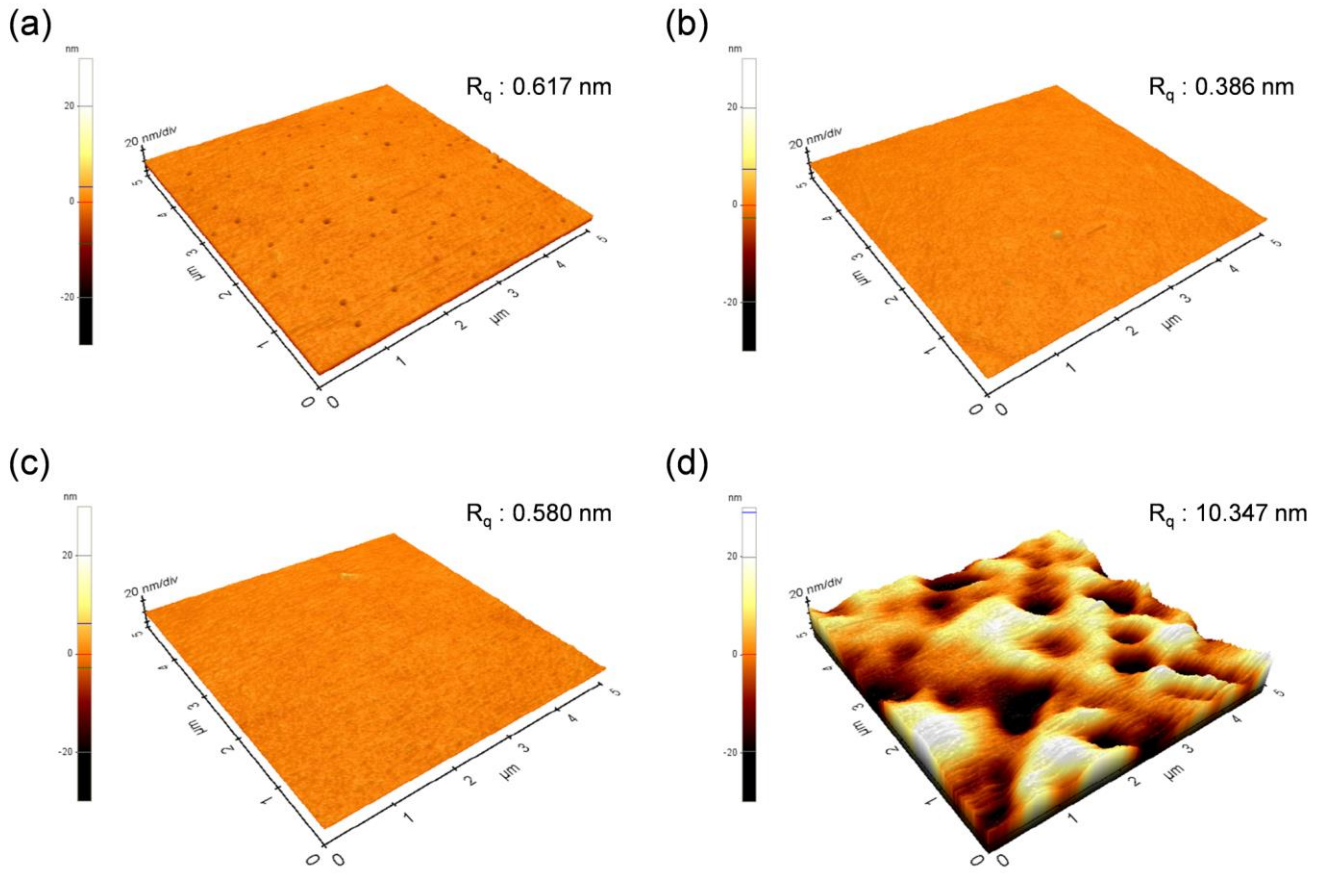

Figure S12. Atomic force microscope (AFM) images of 5 μm × 5 μm area of spin-coated PNB-CBP films doped with (a) **3a**, (b) **3b**, (c) **3c**, and (d) **4** at 8 wt% on quartz substrate.